

Controlled Ground-Borne Vibrations for Design of Sub-structural Systems—Theory and Practice



Deepankar Choudhury , Milind Patil , and Ritwik Nandi 

1 Introduction

In urban areas, underground mass rapid transit systems are becoming popular to fulfill the transportation demand of the public. The construction activities of these transportation systems generate heavy vibrations that propagate through the soils to the ground and create disturbance to nearby buildings and residents. In recent years, ground-borne vibration and their mitigation is receiving much attention from researchers and practitioners. Majority of research work has been conducted on train-induced vibrations, very few studies are available related to excavation or tunneling induced ground vibration. Several researchers used semi-analytical approaches to model ground vibrations induced by underground railway (He et al., 2018; Hussein et al., 2014; Kuo et al., 2011; Yuan et al., 2016, 2017). These are the simplified methods that may not be suitable in engineering practice because of their limitation in simulating geometries. Many researchers have used numerical methods to predict vibration generation and transmission (Amado-Mendes et al., 2015; Galvín et al., 2010; Lopes et al., 2014; Yaseri et al., 2018). However, most of the studies neglected the effect of mechanical process during tunneling. Present and future ground-borne vibration levels are highly depending on the construction method of tunnels. Muller et al. (2008) developed three-dimensional numerical model on a coupling of analytical method and finite element method for both circular and rectangular tunnels.

D. Choudhury (✉) · R. Nandi
Department of Civil Engineering, Indian Institute of Technology Bombay, Mumbai 400076, India
e-mail: dc@civil.iitb.ac.in

R. Nandi
e-mail: ritnandi@iitb.ac.in

M. Patil
IITB-Monash Research Academy, Mumbai 400076, India

AFRY India Pvt. Ltd, Noida, India

Yaseri et al. (2014) used coupled finite element and boundary element methods to predict underground train-induced ground-borne vibration. The scaled boundary finite-element method (SBFEM) was used to model outer media around the tunnel. Patil et al. (2015, 2017, 2018) and Choudhury et al. (2019) investigated the factors affecting the behavior of tunnel under seismically induced vibrations using finite element method. Nandi and Choudhury (2018, 2019, 2021) investigated the effect of earthquake-induced vibration on the behavior of embedded cantilever retaining walls, reinforced soil wall and passive earth pressure. Few researchers used physical modeling approach to study ground-borne vibration problems (Thusyanthan & Madabhushi, 2003; Trochides, 1991; Tsuno et al., 2005). Yang et al. (2013a, b) used centrifuge modeling to study the effects of soil non-homogeneity on propagation of ground-borne vibration. The results show that it is important to consider the soil non-homogeneity of soil in determination of soil dynamic response. Many field measurement studies have also been conducted to investigate the vibration phenomena (Auersch, 2005; Galvín & Domínguez, 2007; Paolucci & Spinelli, 2006).

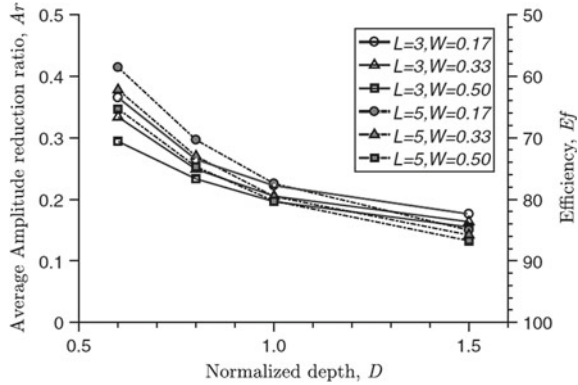
An attempt has been made through this study to provide an insight into theory and practice of controlling ground-borne vibration in sub-structural systems. The open and infill trench methods of vibration mitigation and their efficiency are discussed first. Then the response of multilayer railway track system under cyclic loading is briefly explained. Additionally, a generalized empirical model is explained, this model determines uses basic soil properties to determine the blast-induced vibration parameters. Finally, an emphasis has been given on evaluating the effect of excavation of underground metro station and other related construction activities such as tunneling, blasting, piling, on adjacent structures. Tunneling-induced vibration impact assessment of heritage structure has been explained through a case study.

2 Mitigation of Ground-Borne Vibration

Bose et al. (2018) investigated the use of trenches as a wave barrier in mitigating ground vibration. A numerical model was developed using PLAXIS to study the factors affecting the vibration isolation efficiency of open and infill trenches. Open trench is characterized by three variables: depth (d), width (w) and screening distance (l). These parameters were optimized through parametric study under harmonic loading to achieve maximum screening efficiency. Results of parametric study are plotted in terms of variation of efficiency (amplitude reduction ratio) with change in trench's geometrical parameters. From Fig. 1, it can be observed that normalized depth is a key parameter that controls the efficiency of the isolation system. Efficiency increases with increase in depth. In all the cases of parametric study, the minimum efficiency noted was 55%, whereas maximum was more than 80%. Barrier location and width of trench appear to be the insensitive parameters. Only in case of shallow trenches, the width has played the significant role in blocking wave energy.

At high wavelength, construction and stability of open vertical cuts become difficult. In such cases, infill trenches are more suitable compared to open trenches. In

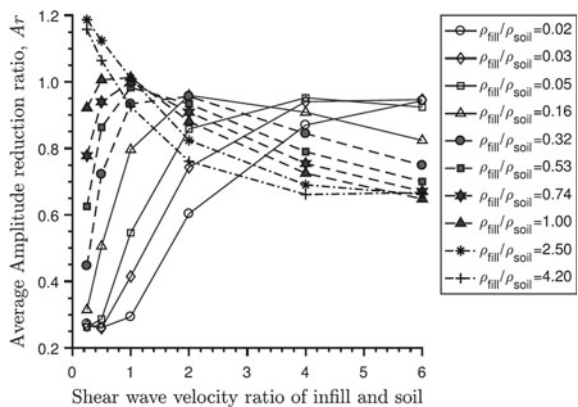
Fig. 1 Variation of average amplitude reduction ratio with depth of an open trench (republished with permission from ASCE, from Bose et al. (2018))



open trench, efficiency is governed by the wave reflection, whereas in infill trenches the combination of reflected and transmitted waves plays the major role. Performance of high-density and low-density materials with varying shear wave velocity is compared through finite element analysis.

Figure 2 shows the variation in the average amplitude ratio with change in shear wave velocity ratio of infill material and in situ material. It can be seen that low-density materials performed well as the wave barriers compared to high-density materials. Moreover, the response of materials depended on the relative shear wave velocity of fill material and in situ soil. Infill trenches showed better efficiency when the shear wave velocity of fill material was less than that of in situ soil. It can be said that the low-density materials possess sufficient energy dissipation capacity. Efficiency of system decreased with an increase in shear wave velocity of fill material. High-density fill materials also performed effectively in mitigating ground vibration. The materials having sufficient stiffness are capable of resisting incoming wave.

Fig. 2 Variation in average amplitude reduction ratio with the shear-wave velocity ratio of fill material and in situ soil (republished with permission from ASCE, from Bose et al. (2018))



3 Response of Railway Track System Under Cyclic Loading

Ballast and subgrade are the most important components of the railway track system, which distribute the large cyclic wheel loads from the wheel to the underlying soil strata. Typical representation of railway track system is shown in Fig. 3. Choudhury et al. (2008) and Bharti et al. (2006) presented analytical model of a multilayered track using 2 degrees of freedom (2DOF) mass-spring dashpot system, as shown in Fig. 4.

Dynamic behavior of both ballast and subgrade layers was investigated using time zone and frequency domain analyses. The subgrade is considered as an elastic half-space, and the ballast is assumed to be an elastic layer, this makes the 2DOF approach

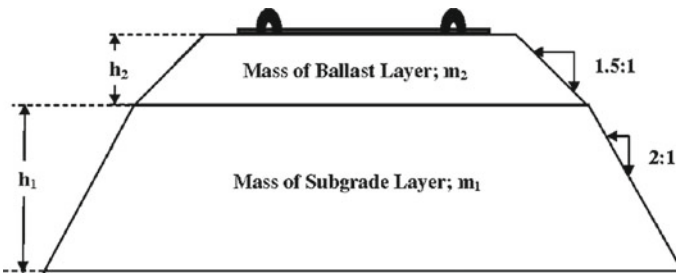
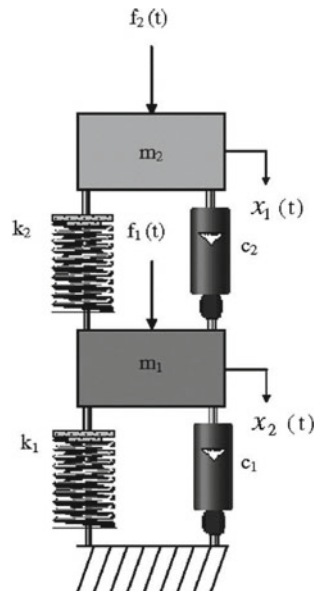


Fig. 3 Typical ballast and subgrade layer below railway track (republished with permission from ASCE, from Choudhury et al. (2008))

Fig. 4 2-DOF MSD mathematical model (republished with permission from ASCE, from Choudhury et al. (2008))



more realistic compared to normal SDOF model. The differential equations of the system have been derived by considering the dynamic equilibrium and D'Alembert's principle. The system of equations obtained is as follows:

$$\begin{bmatrix} m_1 & 0 \\ 0 & m_2 \end{bmatrix} \begin{Bmatrix} \ddot{x}_1 \\ \ddot{x}_2 \end{Bmatrix} + \begin{bmatrix} c_1 + c_2 & -c_2 \\ -c_2 & c_2 \end{bmatrix} \begin{Bmatrix} \dot{x}_1 \\ \dot{x}_2 \end{Bmatrix} + \begin{bmatrix} k_1 + k_2 & -k_2 \\ -k_2 & k_2 \end{bmatrix} \begin{Bmatrix} x_1 \\ x_2 \end{Bmatrix} = \begin{Bmatrix} f_1(t) \\ f_2(t) \end{Bmatrix} \quad (1)$$

The above system of equations can be solved by using Newmark's method. The solutions give the displacement and acceleration response for both the granular and the subgrade layer. The spring stiffness " k_1 " and " k_2 " in the model have been calculated by following equation:

$$k = \frac{0.8(1 - \mu)G}{(1 - 2\mu)h} \quad (2)$$

where,

μ = Poisson's ratio.

G = shear modulus, and.

h = depth of the particular layer.

The equivalent damping coefficients of the dashpots " c_1 " and " c_2 " have been calculated by,

$$c = \sqrt{\frac{2}{1 - \mu}} G \rho \quad (3)$$

where,

ρ = mass density of the layer.

Fundamental circular natural frequency of the ballast and the subgrade has been calculated by,

$$\omega = \frac{\pi v_s}{2h} \quad (4)$$

where,

v_s = shear wave velocity for the medium.

4 Determination of Blast-Induced Vibration Parameters

Kumar et al. (2017) developed empirical relations through random number generation technique. These relations are useful in determining strength parameters of rock, such as Young's modulus, Poisson's ratio, cohesion and angle of friction based on uniaxial compressive strength. Kumar et al. (2016) proposed a methodology for the estimation of engineering properties of soils from field SPT using random number generation. Kumar et al. (2015, 2019) investigated the effects of blast on underground soil media with the help of a finite difference program, FLAC3D.

Kumar et al. (2012a, b, 2014a, b, 2016) proposed model for blast vibration prediction in terms of PPV for a soil site and can be written as,

$$v = kD^{-b} \quad (5)$$

$$D = SD = R/Q^{1/3} \quad (6)$$

where,

D = scaled distance (SD) ($m/kg^{1/3}$).

v = peak particle velocity (PPV) in mm/s.

k and b = site constants.

R = distance from the blast point

Q = charge per delay.

Various combinations of three soil properties, namely, Young's modulus, degree of saturation and unit weight were fitted into linear equations. It was observed that ratio of Young's modulus and unit weight closely fit the linear equation. Based on the collected experimental data, the following generalized empirical relation (with $r^2 = 0.907$) is proposed to evaluate PPV for soil sites.

$$v = \left(\frac{E}{\gamma} \right)^{0.229} D^{-(1.6985-0.175S)} \quad (7)$$

where,

E = Young's modulus of soil.

v = peak particle velocity (PPV) in mm/s.

D = scaled distance (SD) ($m/kg^{1/3}$).

S = degree of saturation.

γ = unit weight of soil.

The performance of proposed model has been investigated by comparing experimental and predicted PPV. The predicted PPV found to be in good agreement with experimentally obtained PPV. For blast-related design, this empirical model can be used in practical applications.

5 Impact Assessment Study of Heritage Structures

The alignment of the proposed metro construction for Phase IV in Delhi, India is passing by few heritage sites (see Fig. 5). The list of the heritage site affecting the metro alignment is listed in Table 1. The metro rail project involves large-scale construction works and other activities at site. There are many construction activities like foundation piling, drilling and blasting, driving, compaction, chiseling, excavation, tunneling (using Tunnel Boring Machine) and such others, which may induce ground vibration and transmission. Hence, a careful assessment of soil–structure interaction and ground-borne vibration transmission to the existing heritage monuments is required. The present study evaluates the effect of ground-borne vibrations on the structures located in the close vicinity of the proposed metro rail alignment. In order to evaluate the adequacy of the proposed metro alignment, the impact assessment of construction activities such as excavation, piling, tunneling and drilling/blasting activities has been carried out on these heritage structures.

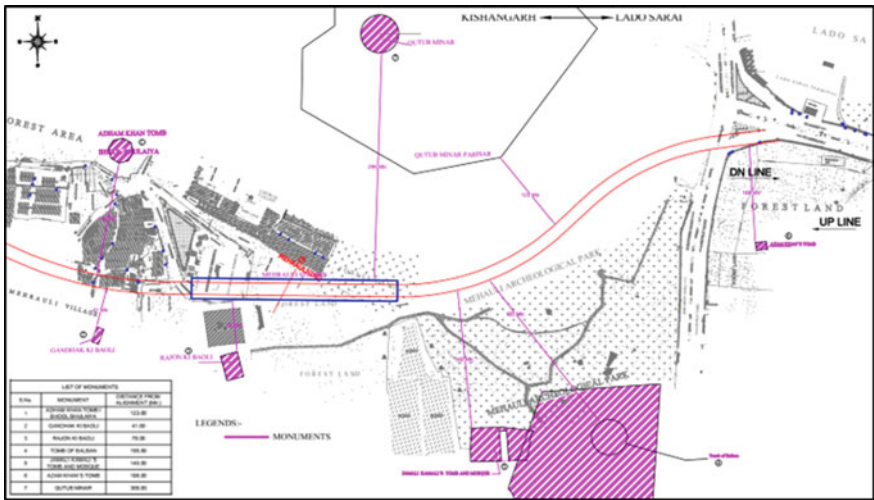


Fig. 5 Layout of the proposed metro line alignment and location of Heritage monuments

Table 1 List of heritage structures in the close vicinity of the proposed metro alignment

Sr. no	Name of heritage monument	Built-in (year)	Distance from the proposed metro alignment (in m)
1	Adham Khan’s Tomb/Bhool Bhulaiya	1562	123
2	Gandhak ki Baoli	1211–1236	41
3	Rajon ki Baoili	1506	78
4	Tomb of Balban	1287	455
5	Jamali Kamali Tomb and Mosque	1528–1529	149
6	Azam Khan’s Tomb	Seventeenth century	108
7	Qutub Minar	1220	300

5.1 Geotechnical Conditions at Site

The deposits in the proposed site location belong to the “Indo Gangetic Alluvium”. Deposits of the Indo-Gangetic Basin are composed of gravels, sands, silts and clays with remains of animal and plants. The geophysical investigation is carried out due to restrictions for drilling of the subsoil in the areas around the heritage site. The layered profile and respective output of seismic refraction test results (in form of compressional wave velocity) are presented in Table 2. In the present analysis, the location of the tunnel section is considered to be at 15 m depth from the ground surface. The investigation results indicate that tunnel is passing through highly weathered rock layer pertaining shear wave velocity (v_s), 400 to 600 m/s.

Table 2 Interpreted stratum based on seismic refraction test

Location	Layer	Depth (m)		Interpreted v_p (m/s)	Interpreted strata
		From	To		
Azam Khan Tomb	1	0	5–12	600–1000	Overburden soil
	2	5–12	30	1500–2500	Rock
ASI Park	1	0	7–8	400–1000	Overburden Soil
	2	7–8	30	1500–3000	Rock
	1	0	8–9	600–1000	Overburden soil
	2	8–9	37	1300–2700	Rock
	1	0	4–8	400–1000	Overburden soil
	2	4–8	25	1300–3500	Rock

5.2 Effect of Ground-Borne Vibration Due to Construction Activity on Heritage Structures

Various sources generate different kinds of ground-borne vibrations that transmit through the soil in different ways, like, transient vibrations, steady-state vibrations and pseudo-steady state vibrations. Vibration can be defined by four parameters: frequency, displacement, velocity, acceleration. Among these variables, the vibration velocity of a particle is directly related to stress generated in the structures, and it is usually measured to evaluate the influence of the vibration on structures. Therefore, the magnitude of vibration is measured in terms of peak particle velocity (PPV). This maximum velocity value, referred to as PPV, is a commonly accepted descriptor for ground vibration amplitude. Given a certain level of vibration, the structural response of a structure to an excitation also depends on its dynamic behavior and in particular of its natural period of frequency. Therefore, predominant frequency is one of the important variables in evaluating the effects of vibration on a structure. The factors that influence the damage to structure subjected to ground-borne vibration are as follows:

- Duration of vibration.
- State of stress to which the structure is subjected.
- Properties of structure, like, foundation type, soil-structure interaction, the quality of materials, the method of construction, and its current state.
- Energy per blow/cycle.
- Distance between source and receiver.

Vibration effects on historic buildings are similar to those for ordinary buildings and structures, although some added complications and uncertainties may be encountered because historic buildings are generally older and may not be structurally as sound as the modern buildings.

5.3 Estimation of Vibration Level Due to Piling Activities

Hiller and Crabb (2000) derived empirical formulae relating resultant PPV with a number of other parameters for vibratory compaction, percussive and vibratory piling, dynamic compaction, the vibration of stone columns and tunnel boring operations from field measurements. These predictions for a variety of scaling factors and parameter ranges are available in BS 5228-2:2009 (British Standard, 2014). Using these formulae, a prediction of resultant peak particle velocities (PPV) can be made conservatively. It suggests that vibration level is practically 0.5 to 1 mm/s for all the cases for the distance more than 30 m.

In the present study, bored piling operation using modern rotary rig is considered and vibration (in the form of PPV) from various distances to the metro rail complex can be calculated from Eq. (8).

$$V_{res} = K_p \left[\frac{\sqrt{W}}{r^{1.3}} \right] \tag{8}$$

where,

W = nominal torque (applied energy in KJ).

K_p = coefficient depends upon soil type (for pile drilling at refusal $K_p = 5$ and for Pile through dense granular soil $K_p = 3$ is considered in the present study).

r = slope distance from the pile toe or tunnel crown, in meters (m).

Though it is recommended to use the slope distance from the point of application of impact/energy to point of interest where resulting vibration V_{res} (in terms of PPV m/s) is to be obtained, in the present study, absolute horizontal plan distance from the metro rail corridor to the Adham Khan tomb is used conservatively. The calculated vibration level is presented in Figs. 6 and 7. Figure 6 represents the situation where piling is carried out at the refusal end, and Fig. 7 represents the situation where piling is carried out through dense gravely/sandy layer. For the drilling through softer layer, the obtained vibration is even lower than these situations due to wave absorption in the softer soils.

Cenek et al. (2012) used correlation (see Eq. (9)) to estimate the magnitude of ground vibrations at any distance from source of construction vibration. This allows estimation of critical separation distances required to ensure that the guideline vibration levels for human comfort and building damage given in BS 5228–2:2009 (British Standard, 2014) and DIN 4150–3:1999 (German Standard, 1999) are not exceeded.

$$V_2 = V_1 \left[\begin{matrix} R_1 \\ R_2 \end{matrix} \right] e^{-\alpha(R_2 - R_1)} \tag{9}$$

Fig. 6 Calculated vibration at various distances due the percussive piling at various frequencies of impact blow (for piles drilled at refusal)

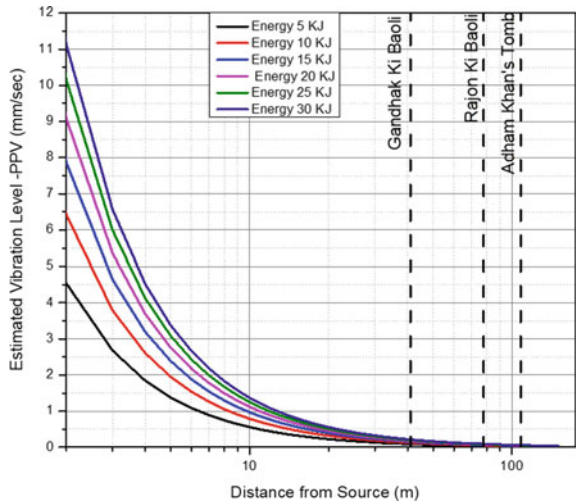
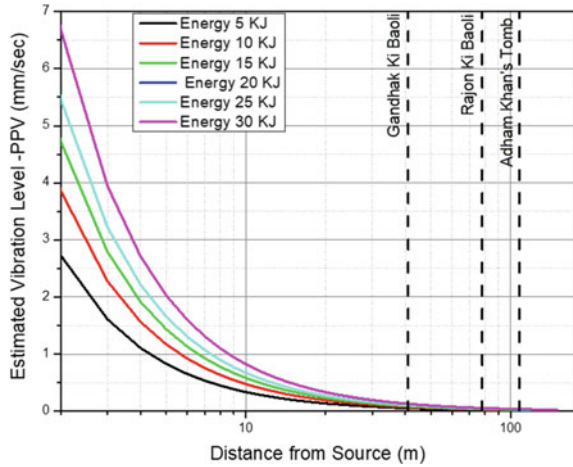


Fig. 7 Calculated vibration at various distances due the percussive piling at various frequencies of impact blow (for piles drilled through dense granular/ sandy stratum or weathered rock)



where,

V_1 = the measured peak particle velocity (mm/s) at distance R_1 (m).

V_2 = the peak particle velocity (mm/s) at distance R_2 (m) from source.

α = soil coefficient for the dominant frequency = $2\pi Df/v_s$.

D = soil damping presently assumed 0.2 on conservative side.

f = frequency of the applied vibration (considered as 10, 20 and 30 Hz).

v_s = shear wave velocity of the soil layers (average along the depth of pile) = 600 m/s conservatively in the weathered rock.

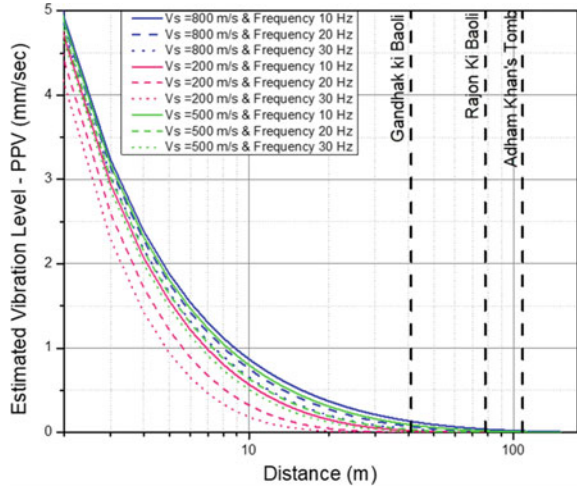
Considering $R_1 = 1$ m and assuming the vibration at the source will be approximately equal to that of a distance of 1 m and considered to be 10 mm/s as given in BS 5228-2:2009 (British Standard, 2014). Eq. (9) is reduced to Eq. (10),

$$V_2 = 10 \left[\frac{1}{R_2} \right] e^{-\alpha(R_2-1)} \tag{10}$$

Considering the frequency of applied vibration as 10, 20 and 30 Hz, respectively, due to rotary piling operation, the calculated peak particle velocity (mm/s) at various distances from 2 to 150 m is presented in Fig. 8.

Based on the threshold vibration PPV recommended by various standards, it is considered that for heritage structure like Adham Khan Tomb, maximum allowed PPV is 2 mm/s. Estimated PPVs are based on above widely followed equations indicate that, in no case, the magnitude of estimated PPVs is close to above 0.1 mm/s. The obtained PPVs from the aforementioned analytical formulations are not transmitted beyond 100 m in all the cases analyzed. In fact, all the estimation suggests

Fig. 8 Calculated vibration at various distances due bored piling (applied vibration PPV 10 mm/s; applied at three different frequencies 10, 20 and 30 Hz, respectively), ($v_s = 800$ represents weathered rock site, $v_s = 500$ represents medium dense soil and $v_s = 200$ represents loose soil profile



that no vibration will be transferred beyond 40 m of the proposed Metro rail corridor. Hence, there is no anticipated vibration at the Adham Khan tomb due to any type of the rotary piling activity at any depth.

In order to investigate the influence of the geotechnical conditions, the variation in the geotechnical profile is considered in the form of variation in the average shear wave velocity of the stratum. Three variations in the shear wave velocity are considered,

- $v_s = 800$ m/s represents weathered rock site.
- $v_s = 500$ m/s represents medium dense soil.
- $v_s = 200$ m/s represents loose soil profile.

From the estimated vibration transmission (PPVs), it is observed that for loose soil profile, the estimated PPVs are lower compared to rock sites. This indicates that considering $v_s = 800$ represents the conservative scenario, where estimated PPVs are higher, and it can be considered to be representative to bored piling activities for the construction of present metro rail complex. Practically, this is in agreement with the geotechnical profile where sound rock is present at shallow depth, that is, 6 m below natural ground level. Table 3 shows the comparison of estimated vibrations at various distances from the vibration source.

5.4 Estimation of Vibration Due to Tunneling

The estimation of ground-borne vibration due to tunneling is carried out using recommendations of BS 5228-2:2009 (British Standard, 2014). The estimated values are presented in Fig. 9. The estimated PPVs at specified sites are as shown in Table 4.

Table 3 Calculated vibration transmission at various distances from vibration source

Distance (m)	Estimated vibration (PPV) at various distances for $v_s = 800$ m/s		
	10 Hz	20 Hz	30 Hz
10	0.868	0.754	0.654
20	0.371	0.275	0.204
30	0.211	0.134	0.085
40	0.135	0.073	0.040
50	0.093	0.043	0.020
100	0.021	0.004	0.001
120	0.013	0.002	0.000

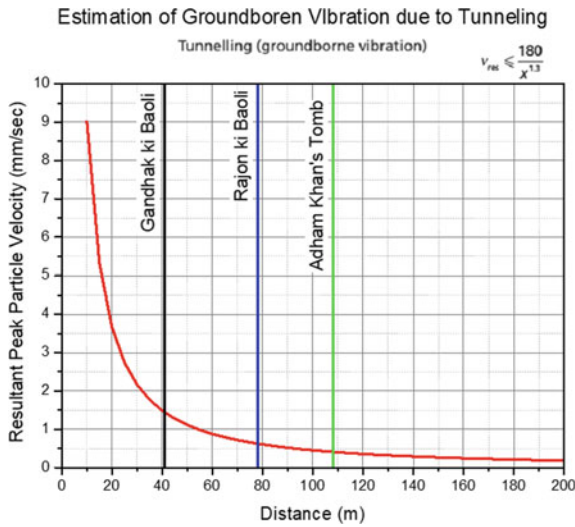


Fig. 9 Obtained ground-borne vibration at various distances due to tunneling

Table 4 Obtained PPVs (peak particle velocity) of vibration originating from tunneling

Sr. no	Name of heritage monument	Distance (m)	PPV (mm/s)	Existing traffic vibration exposure (mm/s)	Total PPV (mm/s)
1	Adham Khan's Tomb/Bhool Bhulaiya	123	0.345	1.230	1.575
2	Gandhak ki Baoli	41	1.441	0.735	2.176
3	Rajon ki Baoli	78	0.625	0.151	0.776
4	Tomb of Balban	155	0.256	0.477	0.733
5	Jamali Kamali Tomb and Mosque	149	0.269	0.357	0.626
6	Azam Khan's Tomb	108	0.409	0.157	0.566
7	Qutub Minar	300	0.108	0.486	0.594

Fig. 10 Charge per delay as a function of range R for safety against damage during underground blasting (Indian Standard, 1973 Adapted from IS 6922)

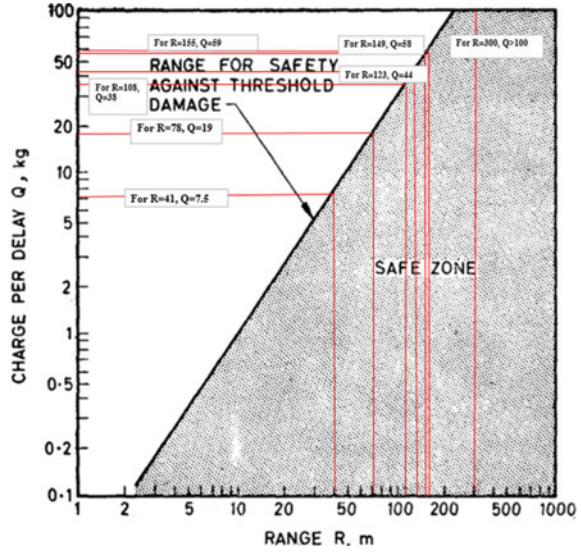


Table 5 Safe distance for blasting as per IS 6922 (Indian Standard, 1973)

Sr. No	Name of heritage monument	Distance (m)	Blast charge per delay (kg)
1	Adham Khan's Tomb/Bhool Bhulaiya	123	44
2	Gandhak ki Baoli	41	7.5
3	Rajon ki Baoili	78	19
4	Tomb of Balban	155	59
5	Jamali Kamali Tomb and Mosque	149	58
6	Azam Khan's Tomb	108	38
7	Qutub Minar	300	100

5.5 Vibration Due to Blasting

IS 6922 (Indian Standard, 1973) specifies the safe distance for blast vibrations. For charge weight up to 100 kg per delay, the safe distance of the structures from the blast point may be obtained from Fig. 10. Safe distances for the various heritage sites have been determined from Fig. 10 and are presented in Table 5.

5.6 Numerical Analysis

A part/section of the proposed Delhi metro line (Phase IV) passing through Mehrauli has been analyzed using numerical simulations to investigate the effect of excavation

of subway station and tunnel driving operations on heritage structures in surrounding area. The construction of proposed metro station (named Mehrauli Metro Station) requires open excavation up to a depth of 15 m from natural ground level. However, such open excavation may induce surface settlement close to the excavation area around the periphery of the proposed metro station. In order to predict possible surface settlement extent and their magnitude, a 3D finite element (FE) analysis was performed using PLAXIS3D v.2017.1.0 (PLAXIS, 2017), a finite element geotechnical computer program. The proposed station is connected to twin tunnels of diameter 6.35 m in both up and down direction. In numerical analysis, tunneling geometry can be simplified into two-dimensional framework considering the infinite length of tunnel in third direction. In order to optimize the computational effort in numerical simulation, twin tunnel excavation is modeled using PLAXIS2D v.2017.1.0 (PLAXIS, 2017). In addition, response of the tunnel-soil system has been examined under seismic loading. A developed 2D FE model was further extended to perform a nonlinear dynamic analysis by applying the acceleration-time history of 1989 Loma Prieta earthquake. As per the soil investigation report, subsoil stratum was divided into three different layers namely sandy silt (0 to 3 m depth), dense sand (3 to 9 m) and quartzite (9 to 40 m), which are modeled using conventional Mohr–Coulomb (MC) constitutive model. The geotechnical properties of each layer adopted in the analysis are given in Table 6. The top soil layer is modeled under drained condition, whereas second and third soil layers are modeled as undrained considering the presence of water table at the 3 m depth from ground level. The proposed station is to be constructed as a cut-and-cover tunnel (of dimensions 270 m in length \times 27 m in width \times 15 m in depth), using top-down excavation method. Excavation depth of 15 m is divided into five-stage process considering layer of 3 m each at a time. The effect of excavation and tunnel driving on surrounding heritage structures has been observed, and the outcomes are reported here.

3D FE analysis of estimation of excavation induced settlements

The soil model of dimensions 950 m \times 600 m \times 40 m has been adopted in the present numerical analysis by discretizing it into 10-noded tetrahedral elements. The horizontal extent of model dimensions was chosen based on the sensitivity analysis to eliminate boundary effects and covering the locations of nearby heritage structures. Standard fixities are assigned wherein the sides are restricted to move laterally, and the base is restrained in all directions. At the bottom of excavation, 300 mm thick PCC layer was laid. All vertical walls of excavation block were secured against lateral deformation by installing diaphragm wall of thickness 800 mm. M40 grade concrete (assuming 70% strength) is used to construct diaphragm wall up to depth of 20 m (15 m excavated portion + 5 m embedded at bottom). Main beams (waling) are provided in the longitudinal direction in the periphery of excavation block at an interval of 5 m. Internal struts were installed in the shorter direction at a center to center distance of 10 m. Figure 11 illustrates the three-dimensional view of the model with dimensions. Figure 12 highlights the excavation portion along with diaphragm wall, waling and struts. The excavation-induced surface subsidence was recorded at different locations, and an attempt has been made to predict the zone of influence

Table 6 Geotechnical material properties

Layer	Thickness (m)	γ_{unsat} (kN/m ³)	E (kN/m ²)	μ	c' (kN/m ²)	ϕ' (°)
1—Sandy silt	3	17	123	0.3	20	22
2—Dense sand	6	19	41	0.25	10	34
3—Quartzite	31	20	300	0.2	55	24

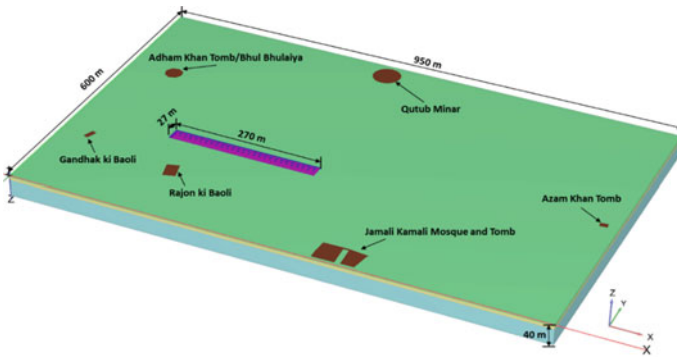


Fig. 11 Three-dimensional view of numerical model used in PLAXIS3D

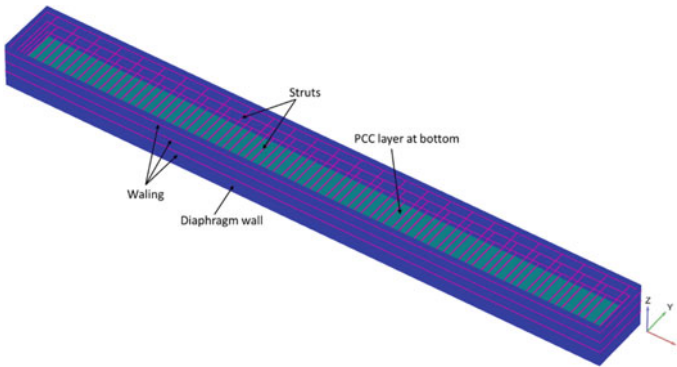


Fig. 12 3D view of excavation portion showing diaphragm walls, waling and struts

around the proposed underground station. Figure 13 demonstrates the surface settlement resulting from the excavation of the proposed station. Displacement contours clearly show that most of the heritage structures are not affected by deep excavation. Only Rajon ki Baoli (indicating displacement of 2.867 mm) may be slightly influenced due to excavation-induced settlements. Controlled excavation operation and proper monitoring can avoid damages to Rajon ki Baoli. The maximum displacement of 13.97 mm was observed in the excavation area, which gets minimized as distance from the excavated pit increases. Figure 14 shows the sectional view of the model cutting across the proposed station and two of the heritage structures, namely, Rajon ki Baoli and Qutub Minar. Displacement contours clearly show that Qutub Minar is located far away from the influence zone of excavation region. However, Rajon ki Baoli may slightly experience the differential settlement that is well within allowable limit. Figure 15 shows the development of plastic zone around excavation pit. However, there are no plastic points/yielding observed in the proximity of any of the heritage structures. The output results in form of displacement are summarized in Table 7.

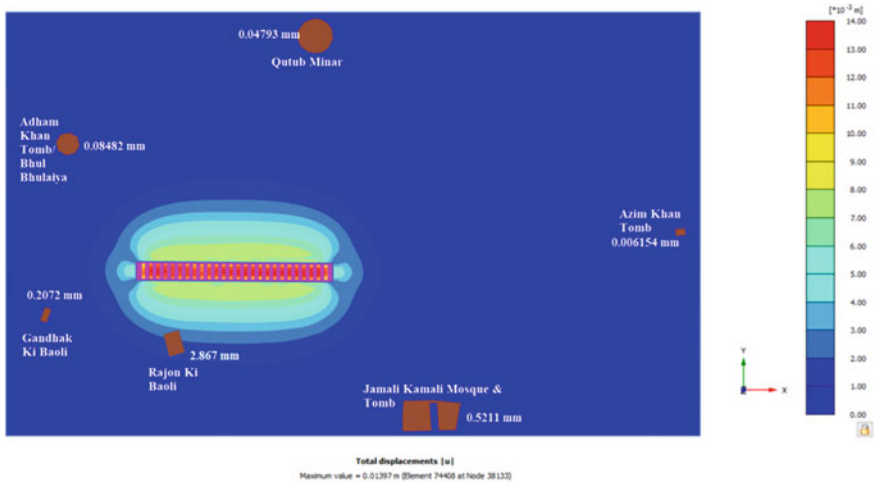


Fig. 13 Final stage displacement contours for the deep excavation for proposed Mehrauli Metro Station

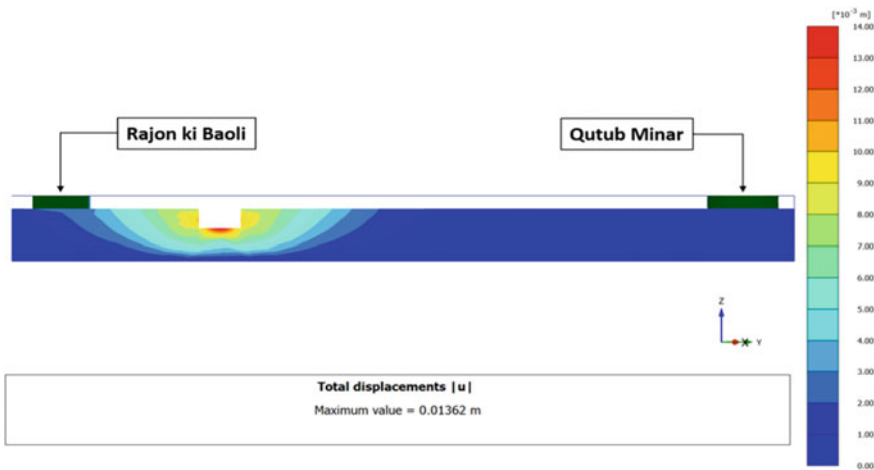


Fig. 14 Section to illustrate the displacement extent around the monuments

2D FE analysis of tunneling operations

The construction of a shield tunnel has been modeled using finite element computer program, PLAXIS2D v2017.1.0. In tunneling process, soil is generally over excavated, which means the cross-sectional area of the final tunnel lining is always less than the excavated soil area. Although measures are taken to fill up this gap, the stress redistributions and deformations in the soil resulting from the tunnel construction process cannot be prevented. To avoid damage to existing buildings and foundations

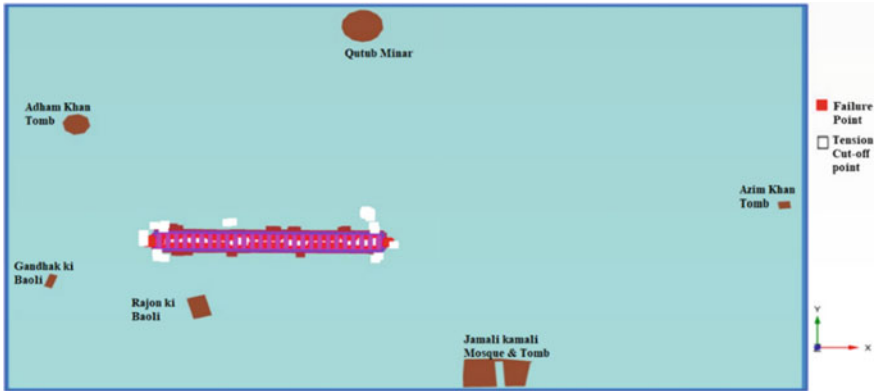


Fig. 15 Accumulation of plastic points around excavation of the proposed Mehrauli Metro Station

Table 7 Obtained phase-wise and total displacements (in mm) for the deep excavation

Monument	Phase displacement (in mm) during each excavation stage of 3 m					Total displacement (mm)
	1st(3 m)	2nd(6 m)	3rd(9 m)	4th(12 m)	5th(15 m)	
Rajon ki Baoli	0.2186	0.5456	0.4760	0.7210	0.7770	2.7382
Gandhak ki Baoli	0.0108	0.0435	0.0379	0.0506	0.0484	0.1912
Adham Khan’s Tomb/Bhool Bhulaiya	0.0068	0.0149	0.0143	0.0206	0.0211	0.0778
Qutub Minar	0.0000	0.0000	0.0000	0.0000	0.0479	0.0479
Jamali Kamali Tomb and Mosque	0.0042	0.0083	0.0081	0.0122	0.0124	0.0453
Azam Khan’s Tomb	0.0000	0.0000	0.0000	0.0000	0.0062	0.0062

resting on the soil above tunnel, it is necessary to predict these stresses and deformations and to take proper measures. A soil model of dimensions 280 m × 40 m has been adopted in the present plane–strain numerical analysis. The twin tunnel of diameter 6.35 m with center-to-center distance of 16 m is located at an average depth of 15 m. The soil profile and geotechnical properties of material are already explained in above section while explaining 3D FE analysis (refer to Table 6). Also, the constitutive material modeling principles of 3D numerical analysis are applicable in 2D FE analysis as well. Tunnel lining (of M45 grade concrete) of thickness 275 mm is modeled using plate element. For more realistic model, simulation of the construction of the tunnel has been defined in a stage-wise process like excavation, contraction, grouting and final lining.

Figure 16 illustrates the developed 2D model in PLAXIS 2D v2017.1.0. Figure 17 shows the sectional geometry and mesh discretization of the 2D FE tunneling model. Twin tunnel has been constructed one after another assuming there is some lag duration in excavating two tunnels in the field. Figure 18 shows the displacement contours resulting from the construction of left tunnel of the twin tunnel. It can be seen from Fig. 19 that as a result of construction of second (right) tunnel there is some

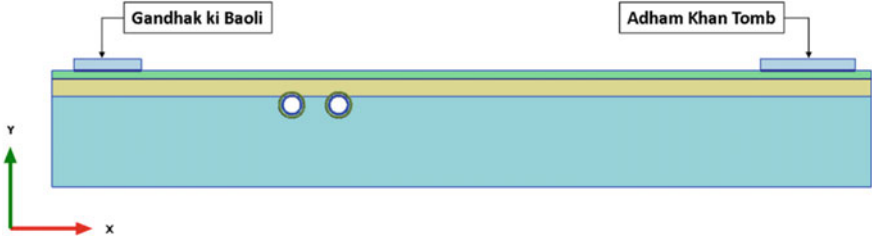


Fig. 16 Two-dimensional view of numerical model used in PLAXIS2D

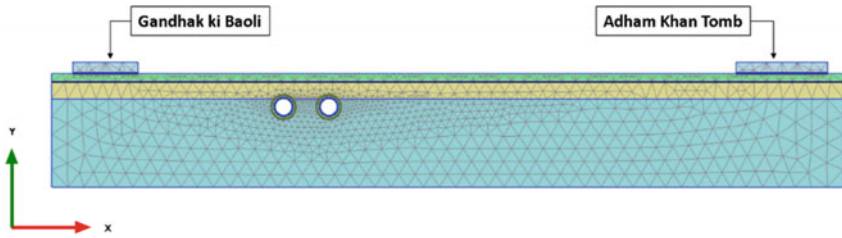


Fig. 17 Sectional geometry and mesh discretization for the 2D FE tunneling model

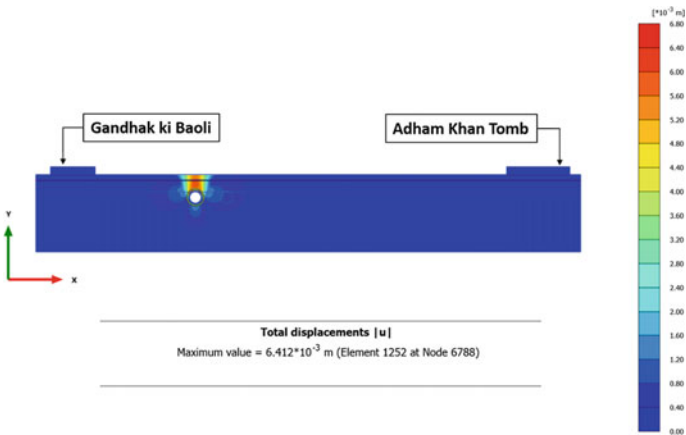


Fig. 18 Displacement contours resulting from the construction of left tunnel of the twin tunnel

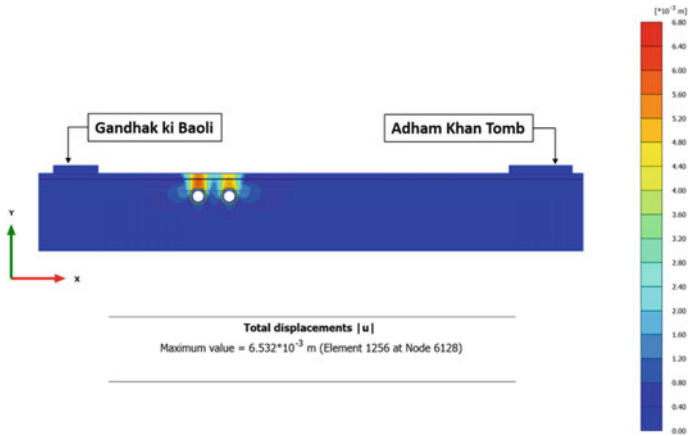


Fig. 19 Displacement contours resulting from the construction of twin tunnel

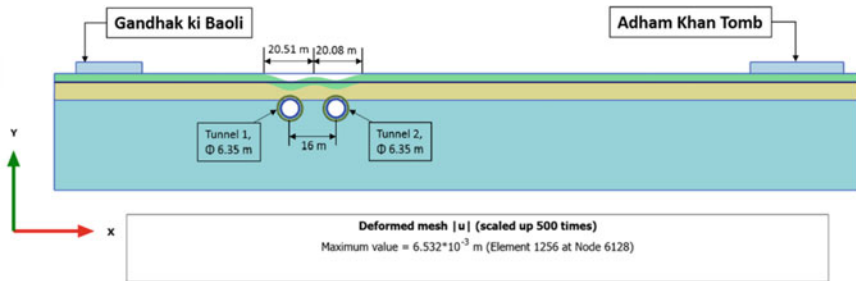


Fig. 20 Tunnel induced surface subsidence due to construction of twin tunnel

settlement of the soil surface. From Fig. 20, the maximum settlement of the tunnel crown is observed to be 6.52 mm and extent of the settlement is limited within the 10 m from the outer periphery of the tunnel. Hence, the tunnel excavation operation or volume contraction due to tunneling will have no significant effect on any of the monument site. Gandhak ki Baoli is the nearest site from the tunnel centerline (i.e. 41 m; refer Fig. 5), and it is observed that settlement due to tunneling is not affecting the closest monument site. The plot of effective stresses (Fig. 21) shows that arching occurs around the tunnel. This arching reduces the stresses acting on the tunnel lining, which in turn lowers the axial force in the final tunnel lining.

5.7 Seismic Analysis of Twin Tunnel

A non-linear dissipative behavior of soil subjected to cyclic loading has been simulated through a plane-strain numerical analysis using PLAXIS2D v2017.1.0. The

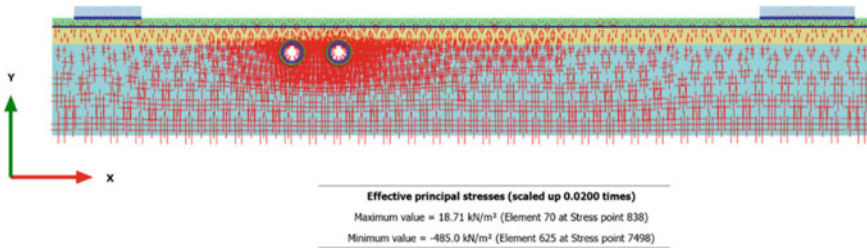


Fig. 21 Effective principal stresses after the construction of the twin tunnel

small size of the numerical model represents the infinite continuous soil medium in reality. An appropriate geometry of the model and boundary conditions were adopted to represent the far-field medium. Already developed 2D FE model of static analysis was further extended to perform non-linear dynamic analysis. Geometric details and geotechnical material properties of the soil as explained in the above section were used in the present seismic analysis. Under earthquake loading conditions, the behavior of the soil is primarily governed by its dynamic properties. Therefore, the shear wave velocity (v_s) was treated as the primary input parameter. The stiffness parameters are calculated from dynamic properties of the soil. During an earthquake, the soil is subjected to cyclic loading and unloading, which generates a hysteresis loop with the dissipation of energy and consequent damping. The Mohr–Coulomb model cannot simulate hysteretic damping in the numerical analysis. To compensate for the modeling limitation in simulating hysteretic damping, the total amount of damping was introduced through the frequency-dependent Rayleigh formulation in terms of viscous damping. The viscous boundary conditions were assigned to vertical boundaries that can absorb the incident waves, and seismic ground motion was assigned to the base of the model. The scaled ground motion data of the Loma Prieta earthquake of 1989 were used as dynamic input motion (see Fig. 22).

Figure 23 shows the location of points where displacements were recorded under the seismic loading. Figure 24 explains the distribution of displacement at various points with respect to dynamic time.

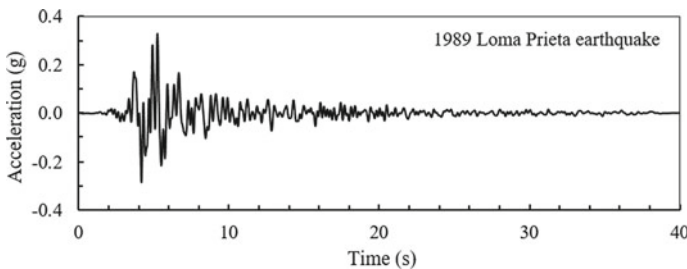


Fig. 22 Acceleration time history of input ground motion (1989 Loma Prieta earthquake)

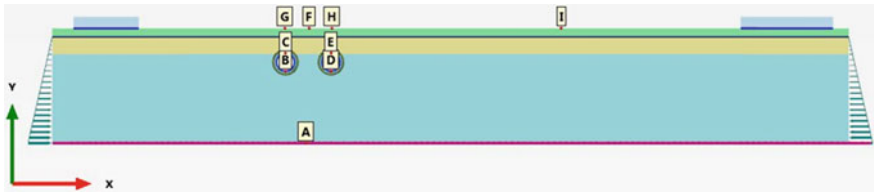


Fig. 23 2D model of seismic analysis with details of observation points

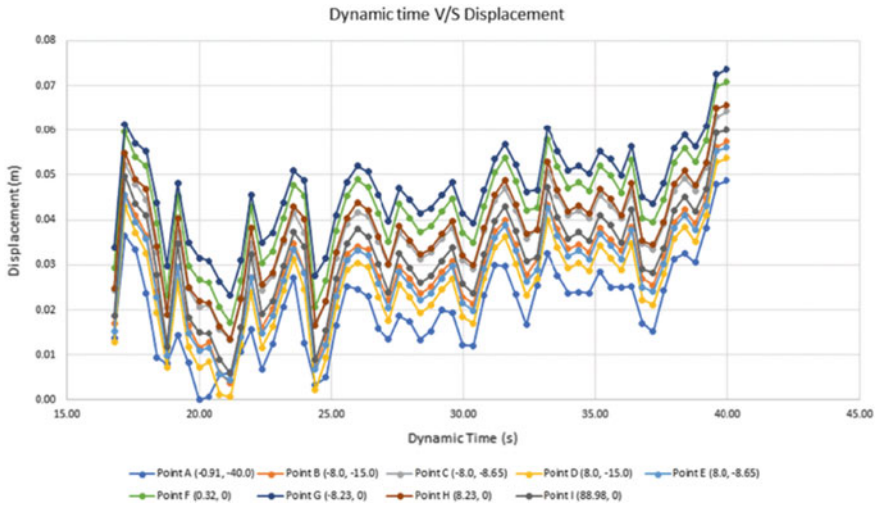


Fig. 24 Plot of displacement versus dynamic time

6 Conclusions

An attempt has been made to provide an insight into theory and practice of evaluation of ground-borne vibration and its control in sub-structural systems. A trenching method of mitigating ground vibration problem discussed and the factors affecting behavior of open and infill trenches have been studied. Optimum values of geometrical and material properties of trenches were determined through parametric study. From results of numerical analysis, it can be concluded that normalized depth is a decisive factor in case of open trenches, whereas width is important in shallow trenches. Performance of the low-density material as an infill material is found out to be exceptionally well but their effectiveness is highly depending on the relative shear-wave velocity between the in situ soil and the infill material. Overall, it is found that the trenches are easy and cost effective solution for controlling ground-borne vibrations. A generalized empirical model has been discussed for estimating blast-induced vibration parameters using extensive experimental data of various sites. This model gives the PPV as a function of scaled distance and three basic soil properties,

namely, unit weight, Young's modulus and degree of saturation. It has been observed that this model predicts reasonably well in case of fully saturated soils irrespective of soil type. Moreover, it predicts higher values for partially saturated soils, in absence of field data, this model can be used to predict vibration parameters by using three basic soil properties.

The behavior of multilayer railway track system subjected to cyclic loading has been explained with the help of analytical approach. The displacement of different layers of railway track systems can be computed using simple 2DOF mass-spring-dashpot system. It can be said that steady-state condition for dense sand achieved much quicker as compared to clay. Dense uniform sand is identified as a most appropriate material for subgrade under cyclic loading because it undergoes least settlement compared to the other soil types.

The vibration transmission due to piling activities (bored piling through rotary boring method) is estimated using widely acceptable empirical equations, and estimated levels are compared with threshold limits recommended by various international standards. Various literatures and standard guidelines were reviewed for identifying the threshold limit of vibration transmission for typical heritage site. The estimated levels of vibration are presented in graphical form, and the estimated vibration is compared for various distances. It is observed that for heritage structures, for all the scale distance from 40 to 100 m, the estimated values are lower than the threshold limit of vibration transmission, that is, 2 mm/s. As per the results of vibration estimation study carried out considering bored piling, it is observed that estimated PPVs are practically nil, and vibration transmission is calculated to be 0.1 mm/s ($\ll 2$ mm/s threshold limit) beyond 50 m distance from proposed location of metro rail complex. Hence, the archaeological structures are at safe distance, and there would be no major vibration impact on these structures due to any type of construction activities. The estimated vertical vibrations are practically zero at the referred distance more than 70 m. However, it is recommended to take precautionary measures during construction for the two sites, namely, Rajon Ki Baoli and Gandhak ki Baoli.

The peak particle velocities due to tunneling were estimated as per recommendations of BS 5228-2:2009. Except Gandhak Ki Baoli, at all the other sites, the estimated PPVs are less than 2 mm/s. Since the threshold limiting value of PPV for heritage structure is considered to be 2 mm/s, the PPV must be restricted within limit during the actual construction process. For rock excavations, blasting charge weights are calculated. It is noted that charge weight should not be exceeded than 7.5 kg at two closest sites, namely, Rajon ki Baoli and Gandhak ki Baoli, to avoid any structural damage due to blasting.

The deep excavation of the proposed Meharauli metro station is modeled numerically using 3D finite element analysis, and influence of the resulting displacements/settlements has been investigated. The estimated maximum settlement is observed to be 2.73 mm at Rajon ki Baoli, which is approximately 78 m away from the proposed excavation footprint. For all other monument sites, the estimated total displacement due to proposed excavation is lower than 1 mm thereby not influencing the structure of the sites. Surface subsidence due to tunneling has been predicted

by 2D numerical analysis. Estimated maximum surface settlement due to tunneling is 6.52 mm above the tunnel centerline, that is, tunnel crown. This surface settlement extent is limited to approximately 12 m from the tunnel centerline towards the monument side, which indicates that monuments are free from any tunneling-induced surface settlement. Additionally, a sample seismic analysis of twin tunnels has been carried out to check the possible displacement caused by seismic shaking.

Acknowledgements Authors want to acknowledge the partial funding received from GeoDynamics vide project number RD/0218-CEGEODS-506 to carry out a portion of the work reported in this paper. Also, a portion of the technical content of this article is reproduced from past literature (Figures) to set the tone of the current study. In accordance, the authors are grateful to American Society of Civil Engineers (ASCE) for granting the permission to reproduce/reuse the appropriate figures in this article.

References

- Amado-Mendes, P., Alves, P., Godinho, L., & Lopes, P. (2015). 2.5D MFS–FEM model for the prediction of vibrations due to underground railway traffic. *Engineering Structures*, *104*, 141–154.
- Auersch, L. (2005). The excitation of ground vibration by rail traffic: Theory of vehicle track-soil interaction and measurements on high-speed lines. *Journal of Sound and Vibration*, *284*(1), 103–132.
- Bharti, R. K., Choudhury, D., & Chauhan, S.: Behaviour of subgrade under cyclic load below railway track. In *Proceedings of Indian geotechnical conference, IGC-2006, December 14–16, 2006, IIT Madras* (pp. 731–7320). Chennai.
- Bose, T., Choudhury, D., Sprengel, J., & Ziegler, M. (2018). Efficiency of open and infill trenches in mitigating ground-borne vibrations. *Journal of Geotechnical and Geoenvironmental Engineering*, *144*(8), 04018048.
- British Standard, BS 5228.2:2009+A1: Code of practice for noise and vibration control on construction and open sites – Part 2: Vibration (2014).
- Cenek, P. D., Sutherland, A. J., & McIver, I. R. (2012). *Ground vibration from road construction*, 485.
- Choudhury, D., Bharti, R. K., Chauhan, S., & Indraratna, B. (2008). Response of multilayer foundation system beneath railway track under cyclic loading. *Journal of Geotechnical and Geoenvironmental Engineering*, *134*(10), 1558–1563.
- Choudhury, D., Patil, M., Ranjith, P. G., & Zhao, J. (2019). Dynamic tunnel-soil interaction in soft soils considering site-specific seismic ground response. In *Frontiers in geotechnical engineering* (pp. 249–271). Springer.
- Galvín, P., & Domínguez, J. (2007). High-speed train-induced ground motion and interaction with structures. *Journal of Sound and Vibration*, *307*(3–5), 755–777.
- Galvín, P., Francois, S., Schevenels, M., Bongini, E., Degrande, G., & Lombaert, G. (2010). A 2.5D coupled FE–BE model for the prediction of railway induced vibrations. *Soil Dynamics and Earthquake Engineering*, *30*(12), 1500–1512.
- German Standard, DIN 4150-3: Structural Vibration – Part 3: Effects of vibration on structures (1999).
- He, C., Zhou, S., Di, H., Guo, P., & Xiao, J. (2018). Analytical method for calculation of ground vibration from a tunnel embedded in a multi-layered half-space. *Computers and Geotechnics*, *99*, 149–164.
- Hiller, D. M., & Crabb, G. I. (2000). Groundborne vibration caused by mechanised construction works. TRL Report 429. Wokingham: TRL (2000).

- Hussein, M., Francois, S., Schevenels, M., Hunt, H., Talbot, J., & Degrande, G. (2014). The fictitious force method for efficient calculation of vibration from a tunnel embedded in a multi-layered half-space. *Journal of Sound and Vibration*, 333(25), 6996–7018.
- Indian Standard, I.S. 6922: Criteria for safety and design of structures subjected to underground blast. Bureau of Indian Standards, New Delhi, India (1973).
- Kumar, R., Choudhury, D., & Bhargava, K. (2012). Response of foundations subjected to blast loadings: State of the art review. *Disaster Advances*, 5(1), 54–63.
- Kumar, R., Choudhury, D., & Bhargava, K. (2013). Recent development in modeling, analysis and design of foundation systems subjected to blast loading considering uncertainties. In *Proceedings of the international symposium on engineering uncertainty: Safety assessment and management (ISEUSAM – 2012b)* (pp. 927–938). Springer, India (2013).
- Kumar, R., Choudhury, D., & Bhargava, K. (2014a). Prediction of blast-induced vibration parameters for soil sites. *International Journal of Geomechanics*, 14(3), 04014007.
- Kumar, R., Choudhury, D., & Bhargava, K. (2014b). Response of shallow foundation in rocks subjected to underground blast loading using FLAC3D. *Disaster Advances*, 7(2), 64–71.
- Kumar, R., Choudhury, D., & Bhargava, K. (2015). Simulation of rock subjected to underground blast using FLAC3D. *Japanese Geotechnical Society Special Publication*, 2(12), 508–511.
- Kumar, R., Bhargava, K., & Choudhury, D. (2016). Estimation of engineering properties of soils from field SPT using random number generation. *INAE Letters*, 1(3–4), 77–84.
- Kumar, R., Choudhury, D., & Bhargava, K. (2016). Determination of blast-induced ground vibration equations for rocks using mechanical and geological properties. *Journal of Rock Mechanics and Geotechnical Engineering*, 8(3), 341–349.
- Kumar, R., Bhargava, K., & Choudhury, D. (2017). Correlations of uniaxial compressive strength of rock mass with conventional strength properties through random number generation. *International Journal of Geomechanics*, 17(2), 06016021.
- Kumar, R., Bhargava, K., & Choudhury, D. (2019). Effect of underground blast on underlying ground media below substructure. In R. Sundaram, J. T. Shahu, & V. Havanagi, (Eds.), *Geotechnics for transportation infrastructure*. Lecture notes in civil engineering (Vol. 28, pp. 363–370). Springer.
- Kuo, K., Hunt, H., & Hussein, M. (2011). The effect of a twin tunnel on the propagation of groundborne vibration from an underground railway. *Journal of Sound and Vibration*, 330(25), 6203–6222.
- Lopes, P., Alves, P., Ferraz, M., Calçada, R., & Silva, A. (2014). Numerical modeling of vibrations induced by railway traffic in tunnels: From the source to the nearby buildings. *Soil Dynamics and Earthquake Engineering*, 61–62, 269–285.
- Müller, K., Grundmann, H., & Lenz, S. (2008). Nonlinear interaction between a moving vehicle and a plate elastically mounted on a tunnel. *Journal of Sound and Vibration*, 310(3), 558–586.
- Nandi, R., & Choudhury, D. (2018). Seismic analysis of reinforced soil wall considering oblique pull-out of reinforcements: A review. *Geotechnical Engineering*, 49(1), 90–98.
- Nandi, R., & Choudhury, D. (2019). Seismic analysis and design of embedded cantilever retaining wall considering non-linear earth pressure distribution effect. In *Earthquake geotechnical engineering for protection and development of environment and constructions* (pp. 4103–4110). CRC Press.
- Nandi, R., & Choudhury, D. (2021). Evaluation of Passive Earth Resistance Using an Improved Limit Equilibrium Method of Slices. *International Journal of Geomechanics*, 21(11), 04021207.
- Paolucci, R., & Spinelli, D. (2006). Ground motion induced by train passage. *Journal of Engineering Mechanics*, *Proceedings of ASCE*, 132(2), 201–210.
- Patil, M., Choudhury, D., Ranjith, P. G., & Zhao, J. (2015). Seismic analysis of tunnels in soft soils: a state-of-the-art review. In: *Proceeding of the international conference on soft ground engineering (ICSGE 2015), 3–4 Dec 2015* (pp. 625–634). Singapore (2015).
- Patil, M., Choudhury, D., Ranjith, P. G., & Zhao, J. (2017). A numerical study on effects of dynamic input motion on response of tunnel-soil system. In *Proceeding of the 16th world conference on earthquake engineering (16th WCEE 2017)*, Paper ID: 3313. Santiago.

- Patil, M., Choudhury, D., Ranjith, P. G., & Zhao, J. (2018). Behavior of shallow tunnel in soft soil under seismic conditions. *Tunnelling and Underground Space Technology*, 82, 30–38.
- PLAXIS 2D v2017.1.0 [Computer software]. PLAXIS BV, Netherlands.
- PLAXIS 3D v2017.1.0 [Computer software]. PLAXIS BV, Netherlands.
- Thusyanthan, N. I., & Madabhushi, S. P. G. (2003). Experimental study of vibrations in underground structures. *Proceedings of Institution of Civil Engineers - Geotechnical Engineering*, 156(2), 75–81.
- Trochides, A. (1991). Ground-borne vibrations in buildings near subways. *Applied Acoustics*, 32(4), 289–296.
- Tsuno, K., Morimoto, W., Itoh, K., Murata, O., & Kusakabe, O. (2005). Centrifugal modeling of subway-induced vibration. *International Journal of Physical Modelling in Geotechnics*, 5(4), 15–26.
- Yang, W. B., Hussein, M. F. M., & Marshall, A. M. (2013a). Centrifuge and numerical modelling of ground-borne vibration from surface sources. *Soil Dynamics and Earthquake Engineering*, 44(1), 78–89.
- Yang, W. B., Hussein, M. F. M., & Marshall, A. M. (2013b). Centrifuge and numerical modelling of ground-borne vibration from an underground tunnel. *Soil Dynamics and Earthquake Engineering*, 51(8), 23–34.
- Yaseri, A., Bazayr, M. H., & Hataf, N. (2014). 3D coupled scaled boundary finite-element/finite-element analysis of ground vibrations induced by underground train movement. *Computers and Geotechnics*, 60(1), 1–8.
- Yaseri, A., Bazayr, M., & Javady, S. (2018). 2.5D coupled FEM-SBFEM analysis of ground vibrations induced by train movement. *Soil Dynamics and Earthquake Engineering*, 104, 307–318 (2018).
- Yuan, Z., Cai, Y., & Cao, Z. (2016). An analytical model for vibration prediction of a tunnel embedded in a saturated full-space to a harmonic point load. *Soil Dynamics and Earthquake Engineering*, 86, 25–40.
- Yuan, Z., Bostrom, A., & Cai, Y. (2017). Benchmark solution for vibrations from a moving point source in a tunnel embedded in a half-space. *Journal of Sound and Vibration*, 387, 177–193.